ISSN 1063-7834, Physics of the Solid State, 2010, Vol. 52, No. 2, pp. 377–383. © Pleiades Publishing, Ltd., 2010.
Original Russian Text © M.V. Gorev, I.N. Flerov, E.V. Bogdanov, V.N. Voronov, N.M. Laptash, 2010, published in Fizika Tverdogo Tela, 2010, Vol. 52, No. 2, pp. 351–357.

LATTICE DYNAMICS AND PHASE TRANSITIONS

Barocaloric Effect near the Structural Phase Transition in the Rb_2KTiOF_5 Oxyfluoride

M. V. Gorev[a, b, *], I. N. Flerov[a, b, **], E. V. Bogdanov[a], V. N. Voronov[a], and N. M. Laptash[c]

[a] *Kirensky Institute of Physics, Siberian Branch, Russian Academy of Sciences, Akademgorodok 50, Krasnoyarsk, 660036 Russia*

* *e-mail: gorev@iph.krasn.ru*

** *e-mail: flerov@iph.krasn.ru*

[b] *Siberian Federal University, pr. Svobody 79, Krasnoyarsk, 660041 Russia*

[c] *Institute of Chemistry, Far Eastern Branch, Russian Academy of Sciences, pr. Stoletiya Vladivostoka 159, Vladivostok, 690022 Russia*

Received June 9, 2009

Abstract—The barocaloric effect (BCE) in the oxyfluoride Rb_2KTiOF_5 has been studied in the vicinity of the structural phase transition at a temperature of 215 K in the pressure range 0–0.6 GPa. It has been established that the extensive and intensive barocaloric effects are $\Delta S_{BCE} \approx -46$ J/kg K and $\Delta T_{AD} \approx 18$ K, respectively, over a wide temperature range 215–280 K. The studies performed have shown that the external hydrostatic pressure is a very effective tool for changing the entropy and temperature of the crystals which undergo structural phase transitions accompanied by a large change in the entropy.

DOI: 10.1134/S1063783410020253

1. INTRODUCTION

Caloric effects of various physical origins in solids and cooling devices based on them have attracted an increased attention of researchers [1, 2]. Generally, these effects are associated with the change in the entropy and temperature of a thermodynamic system when generalized external fields (mechanical stresses, electric, and magnetic fields) vary in isothermal and adiabatic processes, respectively.

The magnetocaloric and electrocaloric effects, which were discovered long ago by Warburg (1881) [3] and Kurtschatov and Kobeko (1930) [4], were for a long time used only in cooling cycles implemented at very low temperatures, where both effects are most pronounced. However, the gradual progress made in the theoretical and experimental methods used for studying magnetothermal and electrothermal properties of materials favored periodic recommencement of interest in studying the magnetocaloric and electrocaloric effects. In recent years, owing to the discovery of significant values of the intensive and extensive caloric effects in the vicinity of phase transitions, the cooling method based on the magnetocaloric and electrocaloric effects are treated as competitive over a wide temperature range, both below and above room temperature [1, 5, 6], with respect to traditional methods based, for example, on the gas and thermoelectric cycles.

It is quite possible that, along with magnetic and electric fields, hydrostatic pressure or uniaxial (compressive or tensile) mechanical stresses leading to the barocaloric (BCE) and piezocaloric (PCE) effects can influence the entropy of a thermodynamic system. The entropy of a solid is the sum of entropies of different subsystems, such as lattice (S_L), electron (S_e), magnetic (S_M), and electrical (S_{EL}) subsystems, and also an anomalous entropy related to phase transitions (ΔS_{an}). All the entropies listed here are to a degree dependent on external pressure, and their changes can contribute to the barocaloric effect. One of the first studies of the barocaloric effect related to pressure-induced modification of the lattice vibration spectrum and, correspondingly, entropy S_L, is associated with the direct measurements of the intensive barocaloric effect in NaCl which is $\Delta T_{AD} \approx 1$ K at room temperature and a pressure of 2 GPa [7]. The barocaloric effect in the region of structural phase transitions was for the first time studied by Müller [3] for $Pr_{1-x}La_xNiO_3$ solid solutions. Since, in these crystals with perovskite-like structure, the displacive transitions occur with a small change in the entropy, the values of the barocaloric effect are very insignificant. It seems likely that the larger the degree of disordering of the structural elements in the initial high-temperature phase of a material, the higher probability of an order–disorder phase transition near the temperature at which a significant barocaloric effect is possible as the temperature decreases.

The barocaloric effect was also studied in materials with other physical mechanisms of changing the

entropy under pressure [8–12]. In some cases, the extensive ΔS_{BCE} and intensive ΔT_{AD} barocaloric effects at pressures below 1 GPa are fairly large and comparable to the changes in ΔS and ΔT in the case of the magnetocaloric effect [8, 9].

In relation to the foregoing consideration, oxyfluoride with the total formula $A_2A'MF_{6-x}O_x$ having an elpasolite–cryolite-type cubic structure (space group $Fm3m$, $Z = 4$) can be promising for obtaining noteworthy parameters of the barocaloric effect. Owing to the possibility of variously combining the contents of the fluorine–oxygen ligands in an anion, a great diversity of structural types of compounds have been created and the statistical disordering of ligands in the crystal lattice provides a means for designing structures with cubic symmetry that undergo phase transitions due to various physical mechanisms and natures [13–15]. The temperature at which the cubic phase in oxyfluorides loses its stability varies over wide ranges depending on the combination of cations. What is most important, the degree of disordering of structural elements in the $Fm3m$ phase of some oxyfluorides is so much significant that the entropy change as a result of the phase transitions can be of the order of $R\ln 8$ and more [16].

In this work, we determined the barocaloric effect in the elpasolite Rb_2KTiOF_5 which, according to [17], at 215 K and atmospheric pressure undergoes the first-order $Fm3m$ ($Z = 4$) $\longrightarrow$ $I4/m$ ($Z = 10$) structural phase transition accompanied by significant variations of the unit cell volume (~1.2%) and the entropy $\Delta S \approx R\ln 8$. The studies of the permittivity of the ceramic samples show that the transition is nonferroelectric. The structure distortion in the phase transition is due to the rotation of all the octahedra around the forth-order axis, distortion of some octahedra, and significant displacement of the Rb atoms. The hydrostatic pressure favors destabilization of the initial cubic phase, which brings about an increase in the phase transition temperature. At the pressure–temperature phase diagram, the boundary between $Fm3m$ and $I4/m$ phases is practically linear, and the pressure coefficient is fairly significant ($dT/dp \approx 110$ K/GPa).

The intensive caloric effect ΔT_{AD} can directly and reliably be measured only in electric and magnetic fields. Various methods are used for this purpose, but adiabatic calorimeter is most reliable device for characterization of ΔT_{AD}; the calorimeter permits one to relatively easily control and really minimize the heat exchange of a sample with the environment, providing adiabatic conditions $S = \text{const}$ of the experiment. It is of particular importance in the case of a small response of the system under study as the electrocaloric and magnetocaloric effects on the action of an external field [18, 19]. In principle, the calorimetric studies can give information also on the extensive caloric effect (ΔS_{CE}) by measurements of the temperature dependence of the heat capacity of a material depending on the field of corresponding nature.

Adiabatic calorimeter is little adequate for studies of the barocaloric effect, since, in this case, a massive autonomic high-pressure chamber is required, whose heat capacity makes a predominant contribution to the heat capacity measured. This circumstance brings about a significant measurement error of the heat capacity (and, correspondingly, the entropy) and makes it impossible to determine the quantity $\Delta T_{AD}(p)$.

Nonetheless, the extensive caloric effect is only indirectly determined from the Maxwell equation

$$\left(\frac{\partial S}{\partial Y}\right)_T = \left(\frac{\partial X}{\partial T}\right)_Y, \quad (1)$$

using the data on the dependences of the generalized coordinate X (volume, magnetization, and polarization) on the temperature and the generalized force Y (pressure, electric and magnetic fields). In the case of the barocaloric effect, relationship (1) is transformed as

$$\left(\frac{\partial S}{\partial p}\right)_T = -\left(\frac{\partial V}{\partial T}\right)_p, \quad (2)$$

and the relationships for the determination of the intensive and extensive barocaloric effects have the form

$$\Delta S(T,p)_{p_1 \to p_2} = -\int_{p_1}^{p_2} \left(\frac{\partial V(T,p)}{\partial T}\right)_p dp, \quad (3)$$

$$\Delta T_{AD}(T,p)_{p_1 \to p_2} = \int_{p_1}^{p_2} \left(\frac{T}{C(T,p)} \frac{\partial V(T,p)}{\partial T}\right)_p dp. \quad (4)$$

Correct calculations of the thermal effect in this case need data on the equation of state (dependence of the volume on temperature and pressure) of a material, which is also a complex experimental problem [7].

In this work, we demonstrate a possibility of determining the intensive and extensive barocaloric effects based on the data on the temperature dependence of the isobaric heat capacity at atmospheric pressure, the pressure–temperature phase diagram, and the dependence of the phase transition enthalpy (entropy) on pressure. The studies were performed on the samples, which were previously used in measurements of the heat capacity at atmospheric pressure [17].

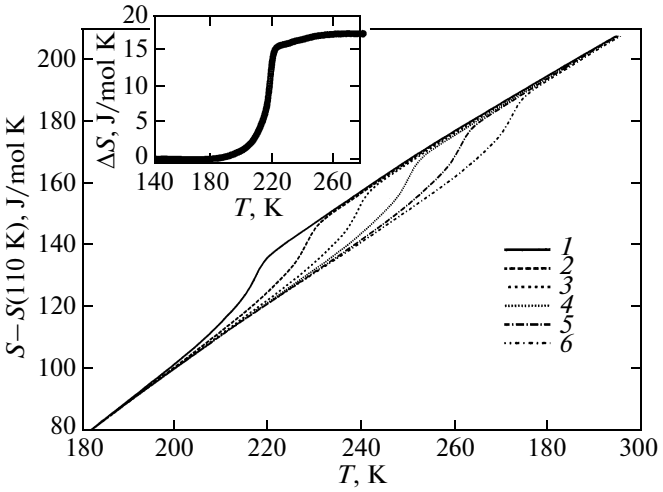

Fig. 1. Temperature dependences of the entropy of Rb_2KTiOF_5 at pressures p = (*1*) 0, (*2*) 0.1, (*3*) 0.2, (*4*) 0.3, (*5*), 0.4, and (*6*) 0.5 GPa. The inset shows the temperature dependence of the anomalous component (ΔS) of the entropy at $p = 0$ GPa [19].

2. BAROCALORIC EFFECT

2.1. Determination of the Barocaloric Effect from the Data on the Heat Capacity and the $p-T$ Phase Diagram

As was mentioned above, the system entropy can be represented as the sum of the contributions of individual subsystems such as lattice, electrons, nuclear spins, anomalous component related to phase transitions, etc. Since, in the Rb_2KTiOF_5 crystal, the ionic bonds are predominant, it seems plausible that the pressure is the main factor which influences the entropy of a structural phase transition. At relatively low pressures under study (0–0.6 GPa), the other entropy components, including the lattice entropy, most likely change insignificantly. Thus, the lattice entropy determined at atmospheric pressure can be used as the background entropy when results of pressure influence are analyzed.

The lattice component of the heat capacity $C_L(T)$ was determined by approximation of the relative heat capacity beyond the region of existence of an anomalous contribution by a combination of the Debye and Einstein functions. The temperature dependences of the lattice entropy (the change in the lattice entropy in the temperature range under study) $S_L(T)$ and anomalous component $\Delta S(T)$ are obtained by integration of $C_L(T)/T$ and $(C_p(T) - C_L(T))/T$, respectively.

The change in the total entropy as a function of temperature and pressure was determined by summation of the lattice component $S_L(T)$ (independent of pressure) of the entropy and the anomalous entropy $\Delta S(T)$. According to the results of studies of the $p-T$ phase diagram, the phase transition temperature (the inflection point in $\Delta S(T)$) is shifted, for each pressure studied, according to the $T_0(p)$ dependence. In this case, it was assumed that, in the pressure range studied (to 0.6 GPa), hydrostatic pressure does not substantially changes the degree of proximity of the phase transition to the tricritical point and, thus, does not change the temperature dependence of the anomalous heat capacity. There are no triple points and pressure-induced phases in the $p-T$ phase diagram [17]. This allows us to assume with confidence that pressure does

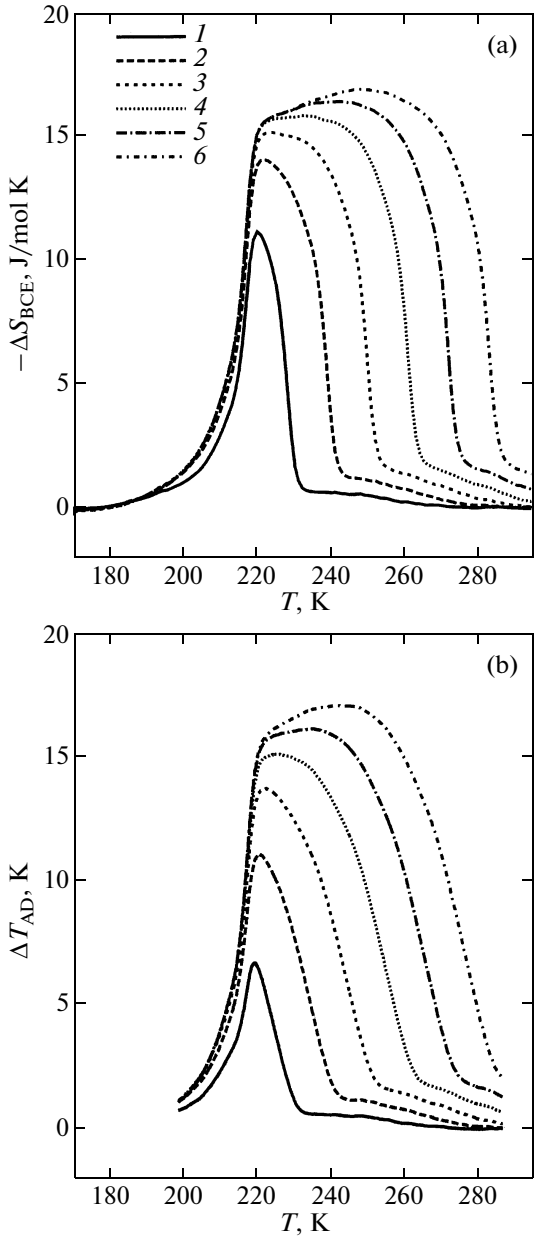

Fig. 2. (a) Extensive ΔS_{BCE} and (b) intensive ΔT_{AD} caloric effects calculated from the data on the heat capacity and dT_0/dp at pressures p = (*1*) 0.1, (*2*) 0.2, (*3*) 0.3, (*4*) 0.4, (*5*), 0.5, and (*6*) 0.6 GPa.

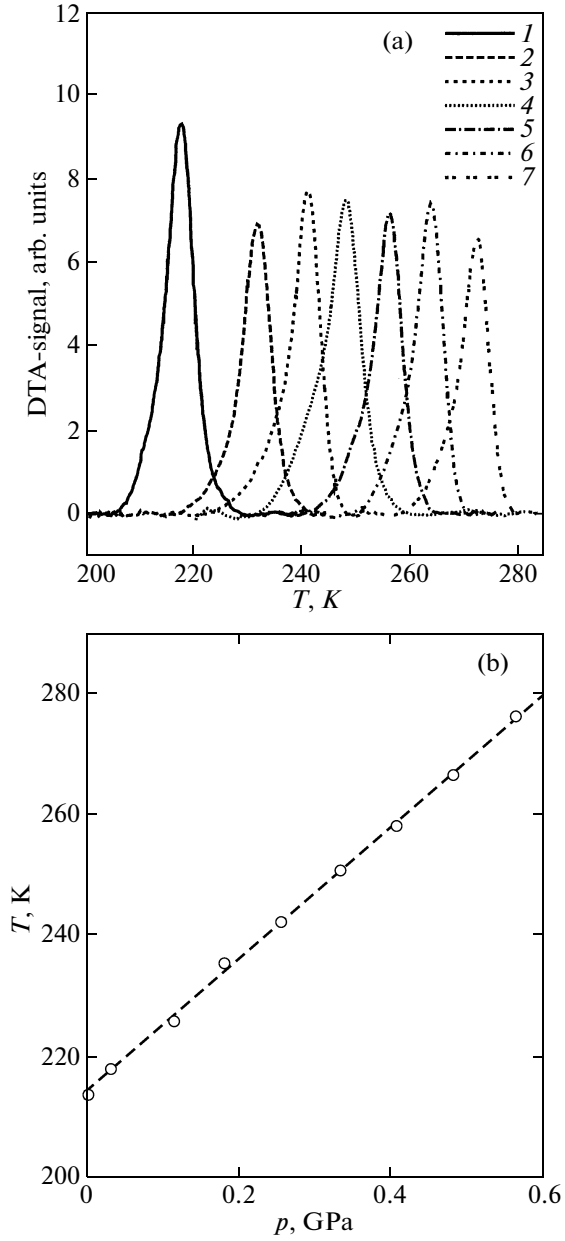

Fig. 3. (a) Anomalous component of the DTA signal at pressures p = (*1*) 0, (*2*) 0.18, (*3*) 0.25, (*4*) 0.33, (*5*), 0.40, (*6*) 0.48, and (*7*) 0.56 GPa. (b) The obtained p–T phase diagram [17].

not change also the phase transition entropy ΔS = 17.3 J/mol K ≈ $R\ln 8$, since the number of possible states of ordering elements before and after the transition is unchanged. Figure 1 shows the dependences of the entropy on temperature and pressure.

Figure 2a depicts the values of the extensive barocaloric effect determined for each pressure as the differences between the entropies under a pressure and at $p = 0$ $\Delta S_{BCE}(T, p) = S(T, p) - S(T, 0)$. As the intensive barocaloric effect is realized at S = const, the $\Delta T_{AD}(T, p)$ dependences were determined using the data on $S(T, p)$ based on the condition $S(T, p) = S(T + \Delta T_{AD}, 0)$ (Fig. 2b).

2. 2. Determination of the Barocaloric Effect from the DTA Studies under Pressure

In order to verify one of the foregoing assumptions that the phase transition entropy is constant in the pressure range studied, we carried out experimental studies of the anomalous component of the entropy and its variation with pressure $\Delta S(T, p)$ using the differential thermal analysis (DTA) in a high-pressure chamber with a multiplier. As a pressure-transmitting medium, we used a mixture of silicon oil and pentane exhibiting optimal properties such as electrical and heat conductivity, solidification point, and viscosity. The pressure was measured by a manganin resistive sensor which has a linear dependence of the electrical resistance on pressure and very small temperature coefficient of resistance, which permits us to neglect, in most cases, insignificant variations of temperature during measurements. Temperature in the high-pressure chamber was measured by a copper–constantan thermocouple calibrated by a standard platinum resistance thermometer. To measure thermal anomalies related to the phase transitions, we used a high-sensitive (~400 μV/K) differential copper–germanium thermocouple which allowed the reliable measurement of even small anomalies of the heat capacity due to both first-order and second-order phase transitions. A quartz bar, as a comparison object, was glued to one of junctions of the differential thermocouple, and a small copper container with the material under study was glued to another junction. The sample mass was ~ 0.1 g.

The typical behavior of the DTA signals at different pressures is illustrated in Fig. 3a, and the obtained p–T phase diagram of the Rb_2KTiOF_5 crystal is shown in Fig. 3b. The temperature dependence of the DTA signal is proportional to the temperature dependence of the anomalous heat capacity $\Delta C_p(T)$ related to the phase transition in the sample under study. It should be noted that all the DTA-signal peaks are practically symmetric with respect to the maximum temperature (the phase-transition temperature) and are characterized by the same fairly narrow temperature range 20–25 K (Fig. 3). This circumstance can be indicative of the absence and broadening of the phase transition and its moving away from the tricritical point under pressure. It is seen that the signal and area under the peak are maximum at $p = 0$. On the other hand, over the pressure range 0.18–0.56 GPa, the parameters under consideration remain constant within the limits of insignificant variations (no more than 10%). The decrease in the parameters at $p \neq 0$ is most likely due to dissipation of a small portion of the transition heat because of an increase in the heat conductivity of the oil–pentane mixture under pressure. Thus, the above assumption that the transition entropy is slightly

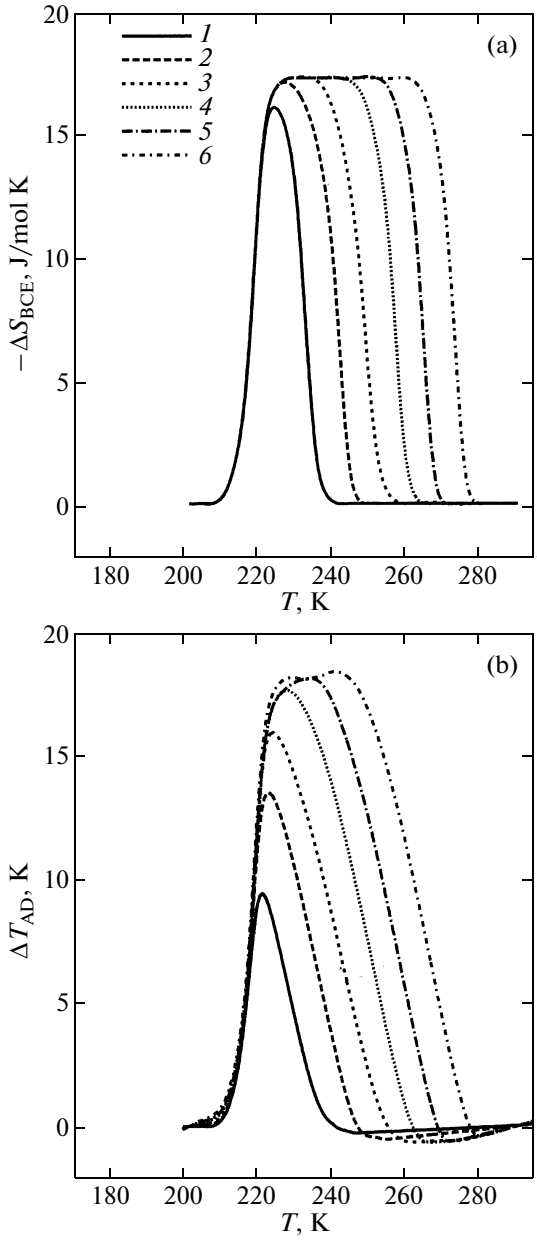

Fig. 4. (a) Extensive ΔS_{BCE} and (b) intensive ΔT_{AD} caloric effects calculated from the data of the DTA studies at pressures $p = (1)$ 0.18, (*2*) 0.25, (*3*) 0.33, (*4*) 0.40, (*5*), 0.48, and (*6*) 0.56 GPa.

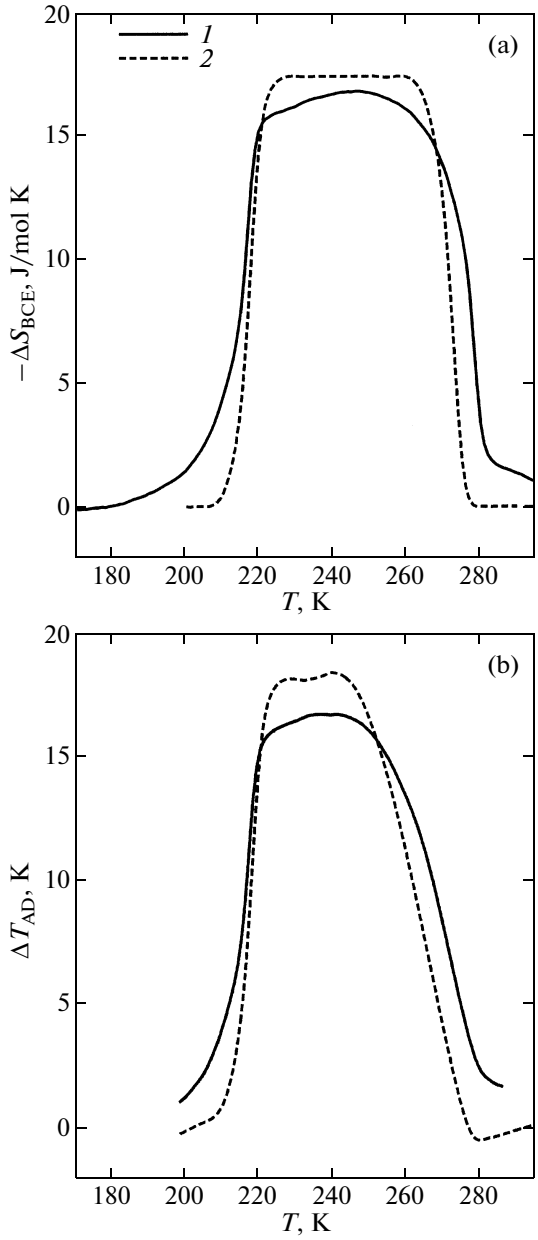

Fig. 5. (a) Extensive ΔS_{BCE} and (b) intensive ΔT_{AD} caloric effects calculated at a pressure $p = 0.56$ GPa from (*1*) data on the heat capacity and dT/dp and (*2*) data of the DTA measurements.

dependent on pressure in the pressure range under study can be justified. This is why the areas under the DTA-signal peaks were normalized to the value of ΔS found from the measurements on the adiabatic calorimeter at atmospheric pressure [17].

The change in the total entropy of Rb_2KTiOF_5 as a function of temperature and pressure was determined by summing the lattice component of the entropy $S_L(T)$ (independent of pressure) and anomalous entropy $\Delta S(T, p)$ found from the DTA measurements and scaled in magnitude on the basis the anomalous entropy obtained from the direct measurements of the heat capacity [17].

The values of the extensive ΔS_{BCE} and intensive ΔT_{AD} barocaloric effects in Rb_2KTiOF_5 determined from the DTA studies are shown in Fig. 4.

Phase transition temperatures T_0 and caloric effects ΔT_{AD} and ΔS_{CE} induced by the magnetic ΔH and electric ΔE fields and by the hydrostatic pressure p (PST–$PbSc_{1/2}Ta_{1/2}O_3$)

Material	T_0, K	ΔT_{AD}, K	ΔS_{CE}, J/kg K	ΔH, kOe	ΔE, kV/cm	p, GPa	ΔT_{eff}, 10^{-2}	References
Pb_2KTiOF_5	215	18	46			0.56	8.4	
$EuNi_2(Si_{0.15}Ge_{0.85})_2$	50	14	39			0.2–0.5	28	[9]
MnAs	312	13	32	50			4.2	[1]
$Gd_5Si_2Ge_2$	280	15	18.5	50			5.4	[20]
PST	290	2.4			138		0.8	[6]

3. DISCUSSION OF THE RESULTS

Comparison of the results obtained by the two methods shows that, in both cases, the maximum magnitudes of the barocaloric effect are approximately the same: $\Delta S_{BCE} \approx 17$ J/mol K = 46 J/kg K and $\Delta T_{AD} \approx 18$ K (Fig. 5). A difference is mainly observed in the $\Delta S(p, T)$ and $\Delta T(p, T)$ dependences (Figs. 2, 4, 5) and it is due to peculiarities of the processes of measuring the heat capacity by method of adiabatic calorimeter and differential thermal analysis. It is seen that, in the former case (Figs. 2a, 2b), the maximum magnitudes of both effects increase by factors of ~1.5 and ~2, respectively, as pressure increases in the range 0.1–0.3 GPa. A further marked decrease in the rate of changing the effects shows that the pressure 0.6 GPa is likely close to the pressure corresponding to the limiting magnitudes of ΔS_{BCE} and ΔT_{AD} in Rb_2KTiOF_5. The character of changes in the barocaloric effects determined by the latter method is somewhat different. The quantity ΔS_{BCE} reaches a value close to the maximum even at 0.18 GPa, while ΔT_{AD} increases gradually, even if more rapidly than in the former case (Figs. 4a, 4b).

The former method is most precise, and the measurements are performed in equilibrium conditions. Unfortunately, the measurements at atmospheric pressure do not allow us to take into account a change in the degree of proximity of the transition to the tricritical point and transformation of the temperature dependence of the heat capacity and, thus, the temperature dependence of the entropy as pressure increases.

The latter method allows us to take into consideration a change in the temperature dependence of the anomalous heat capacity under pressure; however, the measurements are performed in a dynamic (quasi-equilibrium) regime. Moreover, the accuracy of the measurements by the DTA method is significantly lower and it is very difficult to reliably separate the anomalous heat capacity, in particular, far from the phase transition temperature.

Based on the data on the entropy of the phase transition at $p = 0$ and the $p–T$ phase diagram, one can be estimated the maximum barocaloric effects ΔT_{AD}^{max} and ΔS_{BCE}^{max} and pressures at which they are realized. It is natural that the quantity ΔS_{BCE}^{max} is close to the entropy change at the phase transition $\Delta S = R\ln 8 = 17.3$ J/mol K and it is realized, for pronounced first-order transitions, at fairly low pressures. The value of the intensive barocaloric effect ΔT_{AD}^{max} can be estimated from the relationship

$$\Delta T_{AD}^{max} = \Delta S/(dS_L/dT) = \Delta ST/C_L.$$

The value of the lattice heat capacity C_L can be taken from the experimental data [17] or, at temperatures close to the Debye temperature, can be determined using the Dulong–Petit law $C_L \approx 3Rn$, where n is the number of atoms in a molecule (in our case, $n = 10$). The estimated ΔT_{AD}^{max} is 19 K, which is close to that found from analyzing the data of the calorimetric experiments.

The pressure, at which the maximum intensive barocaloric effect can be observed, is determined as

$$p > \frac{T\Delta S}{C_L(dT/dp)} \approx 0.2 \text{ GPa}.$$

This value is lower than the pressures determined experimentally (Figs. 2 and 4), since the transition in Rb_2KTiOF_5 is close to the tricritical point [17].

As mentioned above, there are few data on studies of the barocaloric effect; because of this the table lists the data which allow comparison the caloric efficiency of Rb_2KTiOF_5 with that of ferroelectrics and magnets. Recently, significant values of the electrocaloric effect were obtained in film materials [21]. However, since we studied the bulk sample, the caloric effects were compared with the data obtained for bulk objects. Taking into account that comparison of effects of different physical nature caused by various fields is a fairly subjective, it should be noted, nevertheless, that the oxyfluoride studied exceeds in the values of ΔT_{AD} and ΔS_{CE} the known materials considered as promising coolants, each of which can operate in a certain temperature range.

According to relationship (4), the intensive caloric effect is proportional to temperature. In this connection, it make sense to compare the intensive caloric effects observed in the phase transitions occurring at substantially different temperatures using the effective quantities $\Delta T_{eff} = \Delta T_{AD}/T$. It is seen from the table that $EuNi_2(Si_{0.15}Ge_{0.85})_2$ has the preferable characteristic [9]. On the other hand, the value of ΔT_{AD} in Rb_2KTiOF_5 is close to the maximum values over very wide temperature range (~40 K), unlike other materials.

4. CONCLUSIONS

Based on the analysis of the pressure–temperature phase diagram and the phase transition entropy determined at atmospheric and high pressures using the adiabatic calorimeter and DTA methods, respectively, we calculated the barocaloric effect in the Rb_2KTiOF_5 oxyfluoride, which undergoes a structural transformation. At pressures of 0.3–0.5 GPa, the intensive barocaloric effect $\Delta T_{AD} \approx 18$ K and the extensive barocaloric effect $\Delta S_{BCE} \approx -46$ J/kg K are comparable to the values of the electrocaloric and magnetocaloric effects characteristic of a number of ferroelectrics and magnets considered as promising solid-state coolants.

ACKNOWLEDGMENTS

This study was supported by the Siberian Branch of the Russian Academy of Sciences (Interdisciplinary Integration Project no. 34), the Russian Foundation for Basic Research and the Krasnoyarsk Regional Scientific Foundation within the framework of the "Sibir'" Project (project no. 09-02-98001), and the Council on Grants from the President of the Russian Federation for Support of the Leading Scientific Schools of the Russian Federation (grant no. NSh-1011.2008.2).

REFERENCES

1. A. M. Tishin and Y. I. Spichkin, *The Magnetocaloric Effect and Its Applications* in *Series in Condensed Matter* (Institute of Physics, Bristol, Philadelphia, 2003).
2. J. F. Scott, Science (Washington) **315**, 954 (2007).
3. K. A. Müller, F. Fauth, S. Fischer, M. Kox, A. Furrer, and Ph. Lacorre, Appl. Phys. Lett. **73**, 1056 (1998).
4. P. Kobeko and J. Kurtschatov, Z. Phys. **66**, 192 (1930).
5. V. K. Pecharsky and K. A. Gschneidner, J. Magn. Magn. Mater. **200**, 44 (1999).
6. L. Shebanov, K. Borman, W. N. Lawless, and A. Kalvane, Ferroelectrics **273**, 137 (2002).
7. L. N. Dzhavadov and Yu. I. Krotov, Prib. Tekh. Éksp., No. 3, 168 (1985).
8. Th. Strässle, A. Furrer, A. Donni, and T. Komatsubara, J. Appl. Phys. **91**, 8543 (2002).
9. Th. Strässle, A. Furrer, Z. Hossain, and Ch. Geibel, Phys. Rev. B: Condens. Matter **67**, 054407 (2003).
10. L. G. de Medeiros, N. A. de Oliveira, and A. Troper, J. Appl. Phys. **103**, 113909 (2008).
11. N. A. de Oliveira, J. Phys.: Condens. Matter **20**, 175209 (2008).
12. E. Bonnot, R. Romero, L. Manosa, E. Vives, and A. Planes, arXiv:0802.2009v1 cond-mat.mtrl-sci.
13. G. Peraudeau, J. Ravez, P. Hagenmüller, and H. Arend, Solid State Commun. **27**, 591 (1978).
14. M. Couzi, V. Rodriguez, J. P. Chaminade, M. Fouad, and J. Ravez, Ferroelectrics **80**, 109 (1988).
15. V. D. Fokina, I. N. Flerov, M. V. Gorev, M. S. Molokeev, A. D. Vasiliev, and N. M. Laptash, Ferroelectrics **347**, 60 (2007).
16. I. N. Flerov, V. D. Fokina, A. F. Bovina, and N. M. Laptash, Solid State Sci. **6**, 367 (2004).
17. V. D. Fokina, I. N. Flerov, M. S. Molokeev, E. I. Pogorel'tsev, E. V. Bogdanov, A. S. Krylov, A. F. Bovina, V. N. Voronov, and N. M. Laptash, Fiz. Tverd. Tela (St. Petersburg) **50** (11), 2084 (2008) [Phys. Solid State **50** (11), 2175 (2008)].
18. I. N. Flerov and E. A. Mikhaleva, Fiz. Tverd. Tela (St. Petersburg) **50** (3), 461 (2008) [Phys. Solid State **50** (3), 478 (2008)].
19. A. V. Kartashev, I. N. Flerov, N. V. Volkov, and K. A. Sablina, Fiz. Tverd. Tela (St. Petersburg) **50** (11), 2027 (2008) [Phys. Solid State **50** (11), 2115 (2008)].
20. K. A. Jr. Gschneidne, V. K. Pecharsky, A. O. Pecharsky, V. V. Ivtchenko, and E. M. Levin, J. Alloys Compd. **303–304**, 214 (2000).
21. A. S. Mischenko, Q. Zhang, J. F. Scott, R. W. Whatmore, and N. D. Mathur, Science (Washington) **311**, 1270 (2006).

Translated by Yu. Ryzhkov